JB
Journals.ASM.org

Interaction of the Histone-Like Nucleoid Structuring Protein and the General Stress Response Regulator RpoS at *Vibrio cholerae* Promoters That Regulate Motility and Hemagglutinin/Protease Expression

Hongxia Wang,[a] Julio C. Ayala,[a,b] Jorge A. Benitez,[a] and Anisia J. Silva[b]

Southern Research Institute, Drug Discovery Division, Department of Biochemistry and Molecular Biology, Birmingham, Alabama, USA,[a] and Morehouse School of Medicine, Department of Microbiology, Biochemistry and Immunology, Atlanta, Georgia, USA[b]

The bacterium *Vibrio cholerae* colonizes the human small intestine and secretes cholera toxin (CT) to cause the rice-watery diarrhea characteristic of this illness. The ability of this pathogen to colonize the small bowel, express CT, and return to the aquatic environment is controlled by a complex network of regulatory proteins. Two global regulators that participate in this process are the histone-like nucleoid structuring protein (H-NS) and the general stress response regulator RpoS. In this study, we address the role of RpoS and H-NS in the coordinate regulation of motility and hemagglutinin (HA)/protease expression. In addition to initiating transcription of *hapA* encoding HA/protease, RpoS enhanced *flrA* and *rpoN* transcription to increase motility. In contrast, H-NS was found to bind to the *flrA*, *rpoN*, and *hapA* promoters and represses their expression. The strength of H-NS repression at the above-mentioned promoters was weaker for *hapA*, which exhibited the strongest RpoS dependency, suggesting that transcription initiation by RNA polymerase containing σ^S could be more resistant to H-NS repression. Occupancy of the *flrA* and *hapA* promoters by H-NS was demonstrated by chromatin immunoprecipitation (ChIP). We show that the expression of RpoS in the stationary phase significantly diminished H-NS promoter occupancy. Furthermore, RpoS enhanced the transcription of integration host factor (IHF), which positively affected the expression of *flrA* and *rpoN* by diminishing the occupancy of H-NS at these promoters. Altogether, we propose a model for RpoS regulation of motility gene expression that involves (i) attenuation of H-NS repression by IHF and (ii) RpoS-dependent transcription initiation resistant to H-NS.

Cholera is an acute waterborne diarrheal disease caused by *Vibrio cholerae* of serogroups O1 and O139. This highly motile Gram-negative pathogen continues to be a major public health concern in areas of South Asia and Africa. Infecting *Vibrio* spp. that overcome the gastric acid barrier swim toward the intestinal mucosa and express two major virulence factors: the toxin coregulated pilus (TCP), required for intestinal colonization, and cholera toxin (CT), which is largely responsible for the profuse rice-watery diarrhea typical of this disease (16, 25). Later in infection, *V. cholerae* downregulates the expression of virulence factors and detaches to return to the environment (60). At this stage, the expression of motility and hemagglutinin (HA)/protease has been suggested to facilitate *V. cholerae* detachment from the intestinal mucosa (5, 17, 35, 47). Motility and HA/protease are positively regulated by the cyclic AMP (cAMP)-receptor protein (CRP), which acts by enhancing the quorum-sensing regulator HapR and the general stress response regulator RpoS (4, 29, 46). The expression of both phenotypes is diminished in response to an increase in the intracellular concentration of the second messenger cyclic diguanylate (c-di-GMP) (57).

The histone-like nucleoid structuring protein (H-NS) is a global regulator belonging to a family of small nucleoid-associated proteins that include the factor for inversion stimulation (FIS), the heat-unstable protein (HU), and integration host factor (IHF) (14, 15). Mutations that inactivate *hns* are highly pleiotropic and diminish bacterial growth, suggesting that H-NS influences a broad spectrum of physiological processes (1, 2, 23). H-NS consists of an N-terminal oligomerization domain connected by a flexible linker to a nucleic acid binding domain (2, 8, 14, 36). Both oligomerization and DNA binding are required for the biological activity of H-NS, which includes DNA condensation and the regulation of transcription (10, 50). In transcription regulation, H-NS has been shown to negatively affect gene expression by binding to promoters exhibiting AT-rich highly curved DNA regions that contain clusters of the more conserved 10-bp motif TC GATAAATT (28, 40, 55). In addition, H-NS can positively or negatively affect the expression of a broader spectrum of genes by acting indirectly or binding to mRNA to affect translation (7). A common theme in H-NS transcription regulation is the silencing of horizontally acquired genes (30, 34, 39). Consistent with this role, H-NS has been shown to silence virulence gene expression in *V. cholerae* by acting at different levels of the ToxR regulatory cascade, which includes the *toxT*, *tcpA*, and *ctxA* promoters (37). Further, *V. cholerae hns* mutants have been reported to exhibit diminished motility and intestinal colonization capacity (18, 27, 49, 53). There are numerous evidences indicating that repression by H-NS can be relieved in response to environmental stimuli that activate the expression of other regulators whose binding site overlaps with that of H-NS. For instance, transcriptional silencing of *V. cholerae tcpA* and *ctxA* promoters by H-NS is antagonized by the AraC-like transcriptional regulator ToxT and IHF (51, 52, 59).

The alternative sigma factor RpoS (σ^S) is a global regulator that controls the expression of more than 100 genes in response to

Received 28 July 2011 Accepted 16 December 2011
Published ahead of print 22 December 2011
Address correspondence to Anisia J. Silva, asilva-benitez@msm.edu.

doi:10.1128/JB.05900-11

TABLE 1 Strains and plasmids

Strain or plasmid	Description	Source or reference(s)
Strains		
C7258	Wild type, El Tor biotype, Perú 1991	Clinical isolate
C7258HNS-FLAG	C7258 *hns*::*hns*-FLAG	This study
C7258Δ*lacZ*	C7258 *lacZ* deletion mutant	49
AJB80	C7258 Δ*lacZ* Δ*hns*::Km	49
AJB50	C7258 Δ*rpoS*	29
AJB50HNS-FLAG	AJB50 *hns*::*hns*-FLAG	This study
AJB50Δ*lacZ*	C7258 Δ*lacZ* Δ*rpoS*	49
AJB81	C7258 Δ*lacZ* Δ*rpoS* Δ*hns*::Km	49
C7258Δ*lacZ* RpoS-FLAG	C7258 Δ*lacZ rpoS*::pCVDRpoS-FLAG	This study
AJB80RpoS-FLAG	AJB80 *rpoS*::pCVDRpoS-FLAG	This study
HX120	C7258 Δ*ihfA*	This study
HX121	C7258 Δ*rpoS* Δ*ihfA*	This study
HX120HNS-FLAG	HX120 *hns*::*hns*-FLAG	This study
HX121HNS-FLAG	HX121 *hns*::*hns*-FLAG	This study
Plasmids		
pHNS-FLAG	*hns* ORF cloned in pFLAG-CTC	Sigma-Aldrich
pTT3	*rrnB* T_1T_2 transcription terminator in pUC19	48
pTT3HNS-FLAG	*hns*-FLAG fusion cloned in pTT3	This study
pCVDHNS-FLAG	*hns*-FLAG-*rrnB* T_1T_2 cassette in pCVD442	This study
pKRZ1	Plasmid containing promoterless *lacZ* gene	44
pTT3*flrA*	390-bp *flrA* promoter region cloned in pTT3	This study
pFlrA-LacZ	850-bp fragment containing *rrnB* T_1T_2 and *flrA* promoter in pKRZ1	This study
pTT3*flaA*	450-bp DNA fragment carrying the *flaA* promoter in pTT3	This study
pFlaA-LacZ	890-bp DNA fragment containing *rrnB* T_1T_2 and *flaA* promoter cloned in pKRZ1	This study
pLacZ	Promoterless *lacZ* gene transferred from pKRZ1 to pBR322	This study
pTT4	Transcription terminator *rrnB* T_1T_2 reinserted in pUC19 as a KpnI-BamHI fragment	This study
pTT4RpoN	410-bp DNA fragment carrying the *rpoN* promoter in pTT4	This study
pRpoN-lacZ	DNA fragment containing *rrnB* T_1T_2 and *rpoN* promoter ligated to promoterless *lacZ* gene in pLacZ	This study
pHapLac11	Plasmid vector containing transcriptional *hapA*-*lacZ* fusions	46, 48
pTXB1	Expression vector for construction of in-frame fusions with the intein/chitin binding domain	New England BioLabs
pTXB1-HNS	*hns* ORF cloned in plasmid pTXB1	This study
pTXB1-RpoS	*rpoS* ORF cloned in plasmid pTXB1	This study
pCVDRpoS-FLAG	RpoS-FLAG fusion in suicide vector pCVD442	This study
pUCΔ*ihfA*	0.5-kb SacI-BamHI and 0.5-kb BamHI-SphI fragments flanking *ihfA* sequentially cloned in pUC19	This study
pUCΔ*ihfA*-Km	1.2-kb Km^r gene in BamHI site of pUCΔ*ihfA*	This study
pCVDΔ*ihfA*-Km	SacI-SphI Δ*ihfA*::Km cassette in pCVD442	This study

environmental stresses (20). *V. cholerae rpoS* mutants are more sensitive to starvation, high osmolarity, and oxidative stresses, are less motile than the wild type (WT), and do not express HA/protease (35, 49, 58). We recently reported that RpoS diminishes the cellular concentration of c-di-GMP, an inhibitor of flagellar motility (57). Consistently, microarray studies have shown that *rpoS* mutants express reduced levels of multiple motility and chemotaxis genes, suggesting that *rpoS* could act at an early stage of the motility regulatory cascade (35). In a previous study, we addressed the role of H-NS in the regulation of *V. cholerae* RpoS and RpoS-dependent genes that affect motility and HA/protease production (49). We found that H-NS posttranscriptionally affects RpoS expression in a positive manner, which in turn enhances motility and HA/protease production (49). Accordingly, *hns* mutants were found to be significantly less motile than the wild type and secrete less azocasein activity to the culture medium (49). However, an Δ*rpoS* Δ*hns* double mutant exhibited a slightly larger swarm diameter than the Δ*hns* mutant, suggesting a more complex interplay between H-NS and RpoS in the regulation of motility. In addition, deletion of *hns* in an Δ*rpoS* background resulted in higher expression levels of *flaA*, *flaC*, and *motX* mRNA (49). These results suggested a model in which H-NS can positively affect motility by enhancing RpoS but could also function as a repressor in the absence of RpoS (49). In this study, we further examine the role of H-NS in transcription regulation of motility and HA/protease expression. To this end, we have analyzed the interaction between H-NS and RpoS at the *flrA*, *rpoN*, and *hapA* promoters. We show that H-NS binds to these promoters to repress transcription while RpoS acts to attenuate H-NS transcriptional silencing indirectly by enhancing the expression of IHF and directly by promoting transcription initiation resistant to H-NS.

MATERIALS AND METHODS

Strains and media. The strains, plasmids, and oligonucleotide primers used in this study are listed and briefly described in Tables 1 and 2. Mutants and reporter strains were all derived from *V. cholerae* C7258 (El Tor biotype; Ogawa). *V. cholerae* strains were grown in tryptic soy broth (TSB) with agitation (225 rpm) at 37°C. For cloning purposes, *Escherichia coli* strains TOP10 (Invitrogen) and S17-1λpir (11) were grown in LB medium at 37°C. When necessary, the culture medium was supplemented

TABLE 2 Oligonucleotide primers

Primer name	Sequence (5′→3′)[a]
FlaAp-F	GAAGCATGCCCTTCAATGCCTTATGC
FlaAp-R	GCGAAGCTTGGTCATCGCCGACAC
FlrA-R1	GCTTCCGTGGTCGAGACTTGC
FlrA723	GCCGATGAGCATGCAGGTTAAACT
FlrA884	TCGGGAACACGTTTAAGCGGTAGT
FlrA-R2	GCCCAACAAGGCTACGAAACAG
?>FlrA-R3	TCCGAATTCACACTGCTCTCCTACA
FlrA-F41	GCCGAACCATAAAAATGATCCGCAA
FlrA-R42	CAGGCTAGTTAGTGGCTTCTATTCT
FlrAp-F	GAAGCATGCCTGATCCAAGGTAAG
FlrAp-R	GCGAAGCTTAGTGGCTTCTATTCTATT
HapA-F29	GGTGAATGTATTAAGCGTTGAACCG
HapA-R259	GGTAGGTGTCAAATTTTAAAGGCGC
HNS-F31	GATCGCATATGGTAATGTCGGAAATCACTAAG
HNS-R32	GATCGGCTCTTCAGCACAGAGCGAATTCTTCCAGAGA
IHFA11	AAAGGATCCGTGAGCGCCATAAAACTTCC
IHFA305	GAAGGATCCGTCGAAAAATAAGACCGAGC
IHFA504	GCCGAGCTCCGCAGCAGCGGTAGAGG
IHFA814	TAAGCATGCGGCGAGTCTCGTCACCG
IHFA-F	GATGCCAAGGATACGGTTGAGGTG
IHFA-R	CACGTCGAGCGGTAATAGGAATATC
IHFB-F	AGAAAGACTCTGTGCCGAACAAACG
IHFB-R	TTCCAACTCCACCTTATCGCCAGTC
RecA578	GTGCTGTGGATGTCATCGTTGTTG
RecA863	CCACCACTTCTTCGCCTTCTTTGA
RnnB-F	CGGGGTACCGATTTTCAGCCTGATAC
RnnB-R	CGCGGATCCTGGCTTGTAGATATGAC
RpoN596	CCTTTGGTGTGGCATCGCTTAATC
RpoN875	TGACCAGCCATCGACCTTGTTCTT
RpoN-F21	CCCGATAAAAGTCTTCATCCAGCA
RpoN-R22	GAATTCACGCAAGGTCAGGCATCT
RpoNp-R	CTAGTCTAGATTGGCCGCCAATTTTGAC
RpoNp-F	CGCGGATCCTTTGGGGACATGCAGATC
RpoS1020	CTTCTGCAGTTACTTGTCGTCATCG
RpoS-F11	CCCATATGAGTGTCAGCAATACCGTAACCAA
RpoS-R12	ACGCTCTTCAGCAGTTGTCGTATTCGACGTT
RpsM-F51	GCAACTGCGTGATGGTGTAGCTAA
RpsM-R52	GCTTGATCGGCTTACGCGGACC
TcpA-F1	GTTCATAATTTCGATCTCCACTCCG
TcpA-R2	GTTAACCACACAAAGTCACCTGCAA
VC1922-F61	TAGAAGGTTGACGAAACAAGCAATCA
VC1922-R62	GGTTCAACCACCATAGGTACGAGT
VC2520-F	ATGGGCACTTCACTGTTAGGT
VC2522-F	GGCGATGCTTTGCTGGATGAAC
VC2522-R	CGTTTGAGCCGATAATGTTACCG
VC2522-R1	CACCAATCATCATCGGCAGTTCTCG
VC2522-R2	GGCAATGTTTGAACCGAGGACG
VC2522-R3	AAAGAATTCACCATCATCTCGGGTGCTGAG
VC2523-F	ACTGACGGTGATTTACGGCG
VC2523-R	CAAGAGTTTACGCCCAAGTGC
VC2524-F	CATTACTGGCCGCCGCTCA
VC2524-R	TCCAGTTCGTTACGCGCTTG
VC2525-F	GGGAAATCACTGCACGCAGAG
VC2525-R	CTTTCATCGCTTGACCGTGTG
VC2527-F	CGTCGCAACCTTCTCGCAACT
VC2527-R	CCCTTTGCCATCACTATCGG
VC2528-F	CGCAAACTCTCGGTCGAAGAC
VC2528-R	GCCTTGGCTGACAATATACGC
VC2529-R	GGTTAGATTCCAATGCTTCCTG
VicH5	GGGAAGCTTGTAATGTCGGAAATCA
VicH7	GTTGCATGCATGTCGGAAATCACTA
VicH396	AGGAGATCTCAGAGCGAATTCTTCC
VicH567	GAGTTCCTGCACCTGCTTTTATATG

[a] Restriction sites used for directional cloning are underlined.

with ampicillin (Amp; 100 μg/ml), kanamycin (Km; 25 μg/ml), rifampin (Rf; 150 μg/ml), polymyxin B (PolB; 100 units/ml), isopropyl-β-D-thiogalactopyranoside (IPTG; 20 μg/ml), or 5-bromo-4-chloro-3-indolyl-β-D-galactopyranoside (X-Gal; 20 μg/ml).

Construction of mutants and reporter strains expressing H-NS and RpoS proteins tagged with the FLAG epitope. To construct a strain containing a deletion and Km insertion in *ihfA*, encoding the IHF A subunit, DNA fragments flanking the *ihfA* locus (VC1222) were amplified using primer combinations IHFA504/IHFA11 and IHFA305/IHFA814 and an Advantage 2 PCR kit (BD Biosciences Clontech). The PCR products were sequentially cloned in pUC19 to yield pUCΔihfA. This plasmid was modified by insertion of a Km-resistant cassette from pUC4K (GenBank accession number X06404) to generate pUCΔihfA-Km, and the entire *V. cholerae* DNA harboring the Km-resistant gene replacing the *ihfA* open reading frame (ORF) was transferred to pCVD442 (13) to yield pCVDΔihfA-Km. Finally, the above-mentioned suicide vector was transferred to strains C7258 and AJB50, and mutants HX120 and HX121 (Table 1) were isolated by sucrose selection and confirmed by PCR and DNA sequencing. *V. cholerae* strains expressing H-NS tagged at its C terminus with the FLAG epitope were constructed to conduct chromatin immunoprecipitation (ChIP). To this end, the *hns* ORF (*vicH*, VC1130) lacking the stop codon was amplified from C7258 genomic DNA using primers VicH5 and VicH396. The amplification product was confirmed by DNA sequencing and cloned as a BglII-HindIII fragment in pFLAG-CTC (Sigma-Aldrich) in frame with the FLAG epitope to yield pHNS-FLAG. The H-NS–FLAG fusion was retrieved from pHNS-FLAG by PCR with primers VicH7 and RpoS1020, containing SphI and PstI overhangs, and cloned in pTT3 (48) upstream of the *rrnB* T_1T_2 transcription terminator to yield pTT3HNS-FLAG. The *hns*-FLAG-*rrnB* T_1T_2 cassette was transferred to the suicide vector pCVD442 to yield pCVDHNS-FLAG. Finally, pCVDHNS-FLAG was introduced in strains C7258, AJB50, HX120, and HX121 by conjugal transfer from S17-1λpir to generate strains C7258HNS-FLAG, AJB50HNS-FLAG, HX120HNS-FLAG, and HX121HNS-FLAG, respectively. Exconjugants were selected in LB agar containing Amp and PolB, and correct integration into the *hns* locus was confirmed by PCR using primer VicH567, which anneals to DNA sequences upstream of *hns* not present in pCVDHNS-FLAG, and RpoS1020, which anneals to DNA encoding the FLAG epitope. For strains expressing a chromosomally integrated *rpoS*-FLAG allele from native transcription/translation signals, the suicide vector pCVDRpoS-FLAG (57) was transferred by conjugation to C7258Δ*lacZ* and AJB80 (Table 1). Exconjugants C7258Δ*lacZ* RpoS-FLAG and AJB80 RpoS-FLAG were selected in LB agar containing Amp and PolB, and correct integration within the *rpoS* locus was confirmed by DNA sequencing.

RT-PCR. *V. cholerae* cultures were treated with RNAprotect bacterial reagent (Qiagen), and total RNA was isolated using an RNeasy kit and RNase-free DNase set (Qiagen). Reverse transcription-PCR (RT-PCR) was performed with Superscript III reverse transcriptase (Invitrogen) according to the manufacturer's instructions. Quantitative RT-PCR (qRT-PCR) was conducted using an iScript two-step RT-PCR kit with SYBR green (Bio-Rad Laboratories). Relative expression values were calculated as $2^{(Ct\text{Target} - Ct\text{Reference})}$, where *Ct* is the fractional threshold cycle for the target gene and the reference is the *recA* mRNA. The following primer combinations were used: FlrA723/FlrA884 for *flrA* mRNA, IHFA-F/IHFA-R for *ihfA* mRNA, IHFB-F/IHFB-R for *ihfB* mRNA, RecA578/RecA863 for *recA* mRNA, and RpoN596/RpoN875 for *rpoN* mRNA.

Transcriptional start mapping of the *flrA* and *rpoN* promoters by 5′ RACE analysis. To locate the *rpoN* promoter region, cDNA was synthesized using random hexamers and 20 ng of total RNA. Then, PCRs were carried out using primer combinations consisting of a forward primer annealing to each gene of the putative *rpoN* operon and a reverse primer annealing to the adjacent 3′ open reading frame. A control using total RNA as the template was run for each reaction to exclude chromosomal DNA contamination. Once the *rpoN* promoter region was identified, 5′ rapid amplification of cDNA ends (5′ RACE) was used to determine the

transcription initiation site. Similarly, 5′ RACE was conducted to determine the transcription initiation site of *flrA*. To this end, first-strand cDNA synthesis was conducted using a second-generation 5′/3′ RACE kit (Roche Applied Sciences). Briefly, cDNA was synthesized from 5 μg of total RNA using primer FlrA-R1 for *flrA* and primer VC2522-R1 for *rpoN* as gene-specific primers. The cDNA was treated with RNase H and RNase T1, followed by purification with a High Pure PCR product purification kit (Roche Applied Sciences). Next, cDNA was incubated with terminal transferase for 30 min and the deoxyribosyladenine (dA)-tailed cDNA was amplified with FastStart *Taq* DNA polymerase (Roche Applied Sciences) according to the 5′/3′ RACE kit protocol and by using primers FlrA-R2 and VC2522-R2 for *flrA* and *rpoN*, respectively. Finally, nested PCRs were conducted using each amplified tailed cDNA as a substrate and primers FlrA-R3 and VC2522-R3 for *flrA* and *rpoN*, respectively. The nested PCR products were ligated into SalI- and EcoRI-digested pUC19, and 10 positive colonies were sequenced for each 5′ RACE experiment.

Construction of *flrA*-, *flaA*-, and *rpoN-lacZ* promoter fusions. To construct an *flrA-lacZ* promoter fusion, we amplified a 390-bp fragment containing the *flrA* promoter (as defined by 5′ RACE analysis) with primers FlrAp-F and FlrAp-R. For the *flaA-lacZ* promoter fusion, a 450-bp fragment containing the *flaA* promoter (26) was amplified with primers FlaAp-F and FlaAp-R. In both cases, the promoter fragments were inserted downstream of the *rrnB* T_1T_2 transcription terminator in plasmid pTT3 to generate pTT3*flrA* and pTT3*flaA*, respectively. Then, the terminator-promoter fragment was inserted upstream of a promoterless *lacZ* gene in plasmid pKRZ1 (44) to generate pFlrA-LacZ and pFlaA-LacZ. To construct an *rpoN-lacZ* promoter fusion, we first constructed plasmid pLacZ by ligating a 4.4-kb BamHI-PstI fragment containing the *lacZ* gene from pKRZ1 to a 3.2-kb BamHI-PstI fragment from pBR322. The *rrnB* T_1T_2 transcription terminator was amplified from pTT3 (48) with primers RrnB-F and RnnB-R and reinserted in pUC19 to generate pTT4. Next, a 410-bp fragment containing the *rpoN* promoter region was amplified with primers RpoNp-F and RpoNp-R and inserted in pTT4 to generate pTT4RpoN. Finally, the terminator-promoter fragment was inserted upstream of the promoterless *lacZ* gene in plasmid pLacZ to generate pRpoN-lacZ. The construction of plasmid pHapLac11 containing a *hapA-lacZ* promoter fusion has been described previously (46, 48). The resulting plasmids, pFlrA-LacZ, pFlaA-LacZ, pRpoN-lacZ, and pHapLac11, were introduced into the C7258Δ*lacZ* (WT), AJB50Δ*lacZ* (Δ*rpoS*), AJB80 (Δ*hns*), and AJB81 (Δ*rpoS* Δ*hns*) strains, respectively, by electroporation (31).

Purification of H-NS and RpoS and preparation of polyclonal antibodies. To purify H-NS, the *hns* open reading frame (ORF) was amplified from C7258 genomic DNA using primers HNS-F31 and HNS-R32. The amplified fragment was digested with restriction enzymes NdeI and SapI and ligated into similarly digested pTXB-1 (Table 1) to generate pTXB1-HNS. The H-NS–intein fusion was confirmed by DNA sequencing using T7 universal and Mxe intein reverse primers from New England BioLabs. H-NS was then expressed from the T7 promoter in *E. coli* ER2566 and purified using an Impact kit (New England BioLabs). Briefly, *E. coli* ER2566 containing plasmid pTXB1-HNS was grown in shaken flasks (220 rpm) containing LB supplemented with Amp at 37°C to an optical density at 600 nm (OD_{600}) of 0.3 to 0.4. At this point, the expression of H-NS was induced with IPTG (0.4 mM) and the culture was incubated for 3 h at 29°C. The cells were collected by centrifugation, resuspended in 20 mM Tris-HCl, pH 8.0, 0.5 M NaCl, and 1 mM EDTA, and disrupted by sonication. The cell debris was removed by centrifugation, and H-NS was purified by following the Impact kit protocol. H-NS-containing fractions were combined and dialyzed against 20 mM Tris-HCl, pH 8.0, 1 mM EDTA, and 5 mM sodium citrate at 4°C. The purity of recombinant H-NS determined by SDS-PAGE was found to be higher than 90%. For purification of RpoS, primers RpoS-F11 and RpoS-R12 were used to amplify the *rpoS* ORF. The amplification product was subcloned in plasmid pTXB1 to yield pTXB1-RpoS, and the construct was confirmed by DNA sequencing as described above. Finally, RpoS was expressed and purified as described for H-NS. Custom polyclonal antibody production was conducted at SouthernBiotech (Birmingham, AL). Protein concentrations were determined by the Bradford method, using a Bio-Rad protein assay kit according to the manufacturer's instructions.

EMSA. Electrophoresis mobility shift assays (EMSA) were conducted using a second-generation digoxigenin (DIG) gel shift kit (Roche Applied Sciences). Briefly, the reaction mixtures consisted of 20 mM HEPES, pH 7.6, 1 mM EDTA, 10 mM $(NH_4)_2SO_4$, 1 mM dithiothreitol (DTT), 0.2% Tween 20, 30 mM KCl, 25 ng of calf thymus DNA (Sigma-Aldrich), 3 fmol of DIG-labeled target DNA, and 12 to 48 ng of pure H-NS in a total volume of 20 μl. The binding reaction mixtures were incubated for 20 min at 30°C. Finally, protein-DNA complexes were separated by electrophoresis in 5% Tris-borate-EDTA (TBE) polyacrylamide gels and transferred to nylon membranes, and DNA was visualized using an anti-DIG Fab fragment-AP conjugate, followed by chemiluminescence detection. The following primer combinations were used to amplify the promoter regions under study: FlrA-F41 and FlrA-R42 for *flrA*, HapA-F29 and HapA-R259 for *hapA*, RpoN-F21and RpoN-F22 for *rpoN*, and TcpA-F1 and TcpA-R2 for *tcpA*. The promoter of VC1922, an ortholog of *Salmonella enterica* serovar Typhimurium STM1033 not regulated by H-NS (34), was amplified using primers VC1922-F61 and VC1922-F62.

ChIP. For H-NS promoter occupancy, strains expressing H-NS-FLAG were grown to the stationary phase in TSB medium (16 h). Then, 40 ml of culture was sequentially treated with Rf (20 min, 37°C), 1% formaldehyde (cross-linking, 10 min, 30°C), and 227 mM glycine (30 min, 4°C). Cells were collected by centrifugation, washed twice with phosphate-buffered saline (PBS) supplemented with protease inhibitor cocktail (PIC) and phenylmethylsulfonyl fluoride (PMSF; Roche Applied Science), and divided into aliquots equivalent to 1/(culture OD_{600} reading) ml, and the cell pellets were maintained at −80°C if not processed immediately. Next, the cells were lysed by suspending the frozen pellets in 500 μl of 10 mM Tris-HCl, pH 8.0, 50 mM NaCl containing 20 ng/μl of RNase A, and 10^5 kU of Ready-Lyse lysozyme (Epicentre Biotechnologies), followed by a 30-min incubation at 37°C. One volume of double-strength immunoprecipitation (IP) buffer (200 mM Tris-HCl, pH 7.5, 600 mM NaCl, 4% Triton X-100) containing PIC and PMSF was added to each lysate, and DNA was broken down to a range of 150 to 1,000 bp by sonication. The cell debris was removed by centrifugation, and the lysate was diluted 10-fold in IP buffer. At this stage, a 10-μl input sample was saved as a reference and PCR efficacy control. Protein-DNA complexes were immunoprecipitated by overnight incubation at 4°C with 8 μg of anti-FLAG M2 monoclonal antibody (Sigma-Aldrich) or 8 μg of an unrelated anti-Xpress monoclonal antibody (Invitrogen) for a mock ChIP. The antibody-protein-DNA complexes were pulled down with salmon sperm DNA-treated protein A/G agarose beads (Imgenex, San Diego, CA) for 1 h at 4°C. The beads were washed twice with 100 mM Tris-HCl, pH 7.5, 250 mM LiCl, and 2% Triton X-100, collected in Spin-X centrifuge tube filters (Costar), and washed three times with IP buffer containing 600 mM NaCl, IP buffer, and TE buffer (10 mM Tris-HCl, pH 8.0, 1 mM EDTA). The immunoprecipitated complexes were eluted from the beads by incubation at 65°C for 30 min in TE buffer containing 1% SDS. After reversal of cross-linking (4 h, 65°C), proteins were removed by incubation with 20 μg of proteinase K (1 h, 45°C). Then, immunoprecipitated DNA was purified using a MiniElute PCR purification kit (Qiagen). At least three ChIP assays were conducted for each strain.

Detection of immunoprecipitated DNA. Immunoprecipitated DNA was qualitatively detected by PCR and agarose gel electrophoresis using the primer combinations to amplify the promoter fragments described for the EMSA. Real-time quantitative PCR (qPCR) was used to quantitate promoter occupancy by H-NS. To this end, PCR was conducted using i*Taq* SYBR green supermix with ROX (Bio-Rad). The quantity of immunoprecipitated DNA was calculated as the percentage of the DNA present in the input sample using the formula $IP = 2^{(Ct\text{input} - Ct\text{IP})}$, where *Ct* is the fractional threshold cycle of the input and IP samples. The relative IP was calculated by standardizing the IP of each sample by the IP of the corre-

sponding mock ChIP. Finally, a region within the *rpsM* ORF to which H-NS does not bind acting as a transcriptional repressor was amplified with primers RpsM-F51 and RpsM-R52 and used as a negative control.

Western blot detection of H-NS and RpoS. For detection of native H-NS and RpoS proteins, serum exhibiting high anti-H-NS and anti-RpoS titers was first preabsorbed with crude extracts of *V. cholerae* Δ*hns* and Δ*rpoS* mutants, respectively. To this end, cells were collected by centrifugation at 4°C and resuspended in Tris-buffered saline containing 0.1% Tween 20 (TBST) supplemented with PIC. The cells were disrupted by sonication, and the debris was removed by centrifugation. Then, a 1:1,000 dilution of anti-H-NS or anti-RpoS serum was incubated overnight at 4°C with crude extracts of strain AJB80 (Δ*hns*) or AJB50 (Δ*rpoS*) containing 2 mg/ml protein, respectively. For Western blot analysis, a volume of cells corresponding to 1.0 OD_{600} units was centrifuged and the pellet was resuspended in 0.1 ml of Laemmli's sample buffer (Bio-Rad Laboratories). The cell suspension was placed in a boiling water bath for 10 min, and the cell debris was removed by centrifugation. Proteins were separated using Criterion Precast 10% gels (Bio-Rad) and transferred to polyvinylidene difluoride (PVDF) membranes. The expression of H-NS and RpoS was determined using the corresponding preabsorbed antiserum and horseradish peroxidase (HRP)-conjugated anti-rabbit IgG (Thermo Fisher Scientific, Rockford, IL). A similar procedure was used to detect RpoS-FLAG and H-NS-FLAG but by using monoclonal anti-FLAG M2-peroxidase (Sigma-Aldrich). Membranes were developed using a BM bioluminescence Western blotting kit (Roche Applied Science). To estimate the concentration of H-NS and RpoS in cell lysates, known quantities of each protein were analyzed by Western blotting. Then, a standard curve was constructed for each regulator by plotting band intensities determined using TotalLab Quant software (TotalLab Ltd., Newcastle upon Tyne, United Kingdom) versus concentration.

Enzyme assays. β-Galactosidase activity was measured as described by Miller (33) using the substrate *o*-nitrophenyl-β-D-galactopyranoside. Specific activities are given in Miller units $[1{,}000 \times (OD_{420}/t \times v \times OD_{600})]$, where t is the reaction time and v is the volume of enzyme extract per reaction.

TEM. For transmission electron microscopy (TEM), the cells were pelleted and fixed by reconstitution in 2.5% glutaraldehyde sodium cacodylate buffer, pH 7.3. Samples were adhered to a carbon-coated grid and stained with 1% uranyl acetate before microscopy.

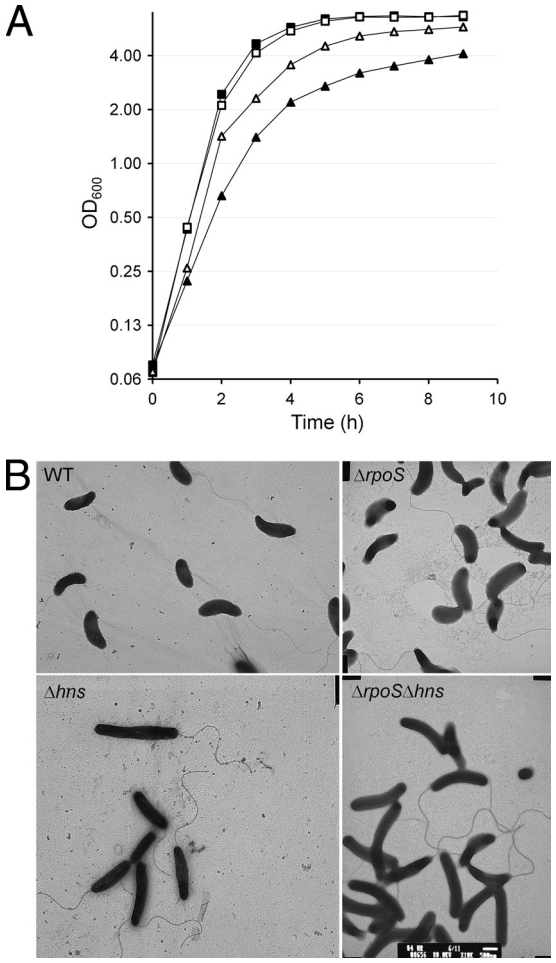

FIG 1 Growth pattern and morphology of *V. cholerae* Δ*hns* mutants. (A) Growth. C7258Δ*lacZ* (WT; □), AJB50Δ*lacZ* (Δ*rpoS*; ■), AJB80 (Δ*hns*; ▲), and AJB81 (Δ*rpoS* Δ*hns*; △) strains were grown with agitation in TSB medium at 37°C, and growth was monitored by measuring the OD_{600}. (B) Transmission electron microscopy. Morphology of C7258Δ*lacZ*, AJB50Δ*lacZ*, AJB80, and AJB81 strains grown to the stationary phase in TSB medium.

RESULTS

Deletion of *rpoS* partially suppresses the slow-growth phenotype of the *hns* mutant. In our previous study, we observed that an Δ*rpoS* Δ*hns* double mutant exhibited a slightly larger swarm diameter than the Δ*hns* single mutant (49). Since differences in growth rate could affect the swarm diameter observed in semisolid agar, we examined the growth patterns of the WT, Δ*rpoS*, Δ*hns*, and Δ*rpoS* Δ*hns* strains. As shown in Fig. 1A, the Δ*hns* mutant exhibited diminished growth compared to the WT and Δ*rpoS* strains. Interestingly, deletion of *rpoS* in the *hns* mutant led to a partial suppression of its slow-growth phenotype. Transmission electron microscopy showed an abundance of elongated cells in the Δ*hns* mutant (Fig. 1B). However, the presence of elongated cells was not suppressed by deletion of *rpoS* (Fig. 1B). It is noteworthy that both the Δ*hns* and Δ*rpoS* Δ*hns* mutants were flagellated but still appeared similarly depressed for motility by hanging-drop bright-field microscopy examination.

The finding that deletion of *rpoS* partially suppressed the slow-growth phenotype of an Δ*hns* mutant suggested that, as observed in *E. coli*, H-NS acts as a repressor of many RpoS-dependent genes (3). Thus, we used specific H-NS and RpoS antisera to measure the expression of these regulators at different stages of the bacterial growth curve. As shown in Fig. 2, H-NS can be detected in both exponentially growing and stationary-phase cultures, while RpoS was induced in the late logarithmic phase ($OD_{600} \geq 2$). Thus, we decided to use cells in the stationary phase (expressing both proteins) for subsequent studies on the interaction between these global regulators.

Regulation of the *flrA*, *rpoN*, *hapA*, and *flaA* promoters by RpoS and H-NS. Microarray studies have shown that deletion of *rpoS* results in reduced expression of motility and chemotaxis genes belonging to the class II, III, and IV hierarchies (35). Therefore, we chose to examine the role of RpoS and H-NS in the transcription of the upstream *rpoN* and *flrA* regulator genes. To specifically address the effect of RpoS and H-NS on the *rpoN* and *flrA* promoters, we determined the transcription initiation sites of both genes and constructed *lacZ* promoter fusions.

The *rpoN* gene is predicted to be part of a large operon, suggesting that it might lack its own promoter (26). By using RT-PCR and different primer combinations, we found that the *rpoN* promoter is located in the intergenic region between VC2520 and VC2522 (data not shown). We then used 5′ RACE analysis to determine the transcription initiation site of *rpoN* and its cognate

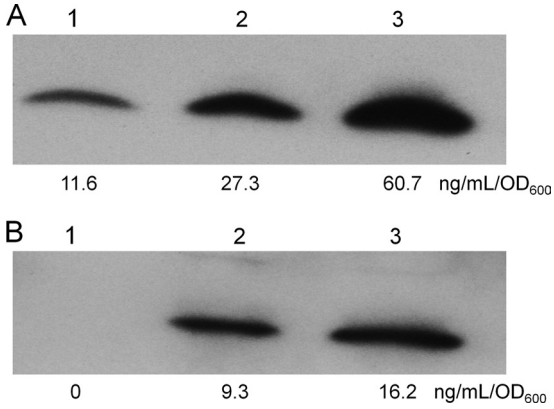

FIG 2 Detection of H-NS (A) and RpoS (B) expression levels. The *V. cholerae* C7258Δ*lacZ* strain was grown in TSB medium, and samples were withdrawn for analysis in the log phase (OD_{600}, 0.5) (lane 1), late log phase (OD_{600}, 2.0) (lane 2), and stationary phase (4 h after the culture reached an OD_{600} of 2.0) (lane 3). H-NS and RpoS protein concentrations are shown below the bands.

σ^{54}-dependent activator *flrA*. Sequencing of the 5′ RACE 500-bp nested PCR product amplified using primer VC2522-R3 indicated that *rpoN* transcription is initiated at a cysteine located 277 bp upstream of the start codon of VC2522. Further, sequencing of the 5′ RACE 250-bp nested PCR product amplified using primer FlrA-R3 indicated that *flrA* transcription is initiated at a cysteine located 146 bp upstream of the *flrA* start codon. Based on this information, we constructed *lacZ* fusions consisting of the *rpoN* and *flrA* promoters linked to a promoterless *lacZ* gene. A similar fusion consisting of the RpoS-dependent *hapA* promoter linked to a promoterless *lacZ* gene has been described previously (48). Expression of the above-noted *lacZ* fusions were examined in the WT, Δ*rpoS*, Δ*hns*, and Δ*rpoS* Δ*hns* genetic backgrounds. As shown in Fig. 3, transcription of *rpoN*, *flrA*, and *hapA* was diminished in the Δ*rpoS* mutant while deletion of *hns* enhanced their transcription. However, *flrA* and *rpoN* differed from *hapA* in that the first two promoters were less dependent on RpoS but more strongly repressed by H-NS. The expression of *flrA* and *rpoN* in the absence of both H-NS and RpoS reflects the level of unrepressed transcription initiation by RNA polymerase (RNAP) containing σ^{70}, which was negligible in the case of *hapA*. We also examined the effect of the regulation on the expression of *flaA*, a gene belonging to the downstream class III transcription hierarchy encoding the major *V. cholerae* flagellin (Fig. 3). As predicted, regulation of *flaA* in stationary-phase cultures followed the same pattern as that of its upstream regulators RpoN and FlrA.

H-NS binds to the *flrA*, *rpoN*, and *hapA* promoters *in vitro*. Our results suggested that H-NS negatively affects the transcription of *rpoN*, *flrA*, and *hapA*. Therefore, we decided to examine whether pure H-NS can bind to these promoters. H-NS is known to bind DNA with a more relaxed sequence specificity than that of other regulators that have more-stringent binding requirements. Thus, we used the *tcpA* promoter, a gene silenced by H-NS (37), and the region upstream of VC1922 as positive and negative controls, respectively. VC1922 is an ortholog of *Salmonella* STM1033 located in a chromosomal region not occupied by H-NS, as described previously in a ChIP-on-chip study (34). We used qRT-PCR to confirm that this gene is also not affected by H-NS in *V. cholerae* (data not shown). As shown in Fig. 4, H-NS was found to bind to the *tcpA*, *flrA*, *rpoN*, and *hapA* promoters while very little binding to the VC1922 promoter could be detected.

RpoS negatively affects H-NS promoter occupancy. To determine H-NS occupancy at the *flrA*, *rpoN*, and *hapA* promoters at the cellular level, we constructed strains C7258HNS-FLAG and AJB50HNS-FLAG (Table 1) and conducted ChIP. In these experiments, we used two negative controls: (i) a DNA sequence located within an ORF of the housekeeping gene *rpsM* and (ii) the promoter region of VC1922, to which H-NS failed to exhibit signifi-

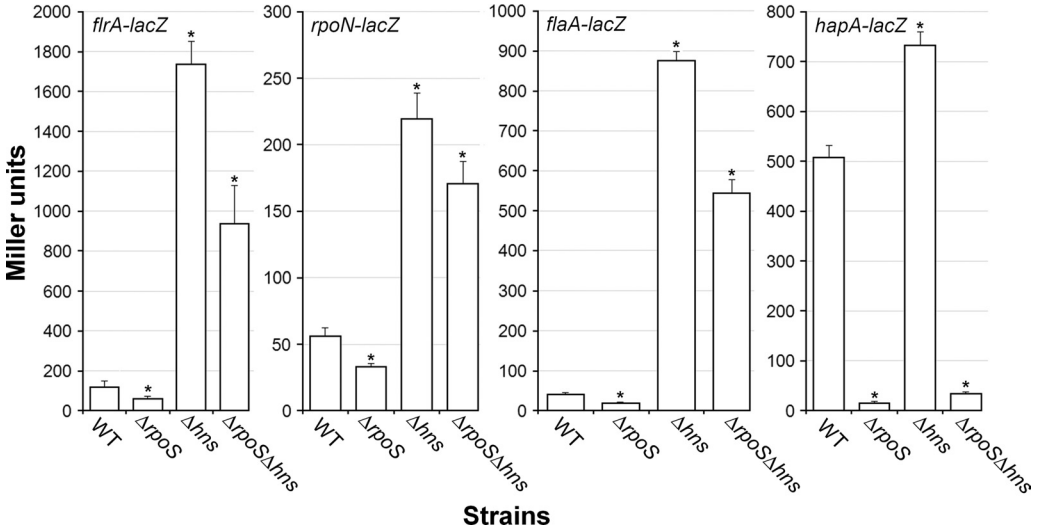

FIG 3 Expression levels of *flrA*-, *rpoN*-, *flaA*-, and *hapA*-*lacZ* promoter fusions in *V. cholerae* Δ*rpoS* and Δ*hns* mutants. C7258Δ*lacZ* (WT), AJB50Δ*lacZ* (Δ*rpoS*), AJB80 (Δ*hns*), and AJB81 (Δ*rpoS* Δ*hns*) strains containing *flrA*-, *rpoN*-, *flaA*-, and *hapA*-*lacZ* promoter fusions were grown to the stationary phase in TSB at 37°C. Detection of β-galactosidase activity was measured as described in Materials and Methods and expressed in Miller units. Each value is the mean for six independent cultures. The error bars indicate standard deviations (*, significantly different from that of the wild type [$P < 0.01$ by a one-tailed *t* test]). The spans of the promoter fragments used relative to the start codon were as follows: positions −536 to −142 for *flrA*, positions −685 to −273 relative to VC2522 for *rpoN*, positions −407 to +43 for *flaA*, and positions −410 to +3 for *hapA*.

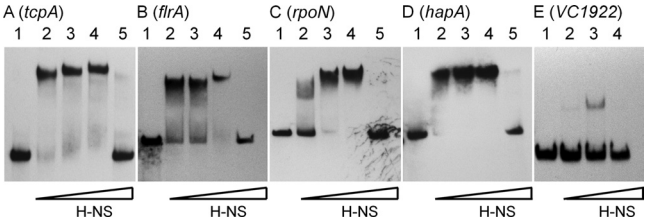

FIG 4 Binding of H-NS to the *tcpA*, *flrA*, *rpoN*, and *hapA* promoters. DIG-labeled DNA fragments encoding the *tcpA* (A), *flrA* (B), *rpoN* (C), *hapA* (D), and VC1922 (E) promoters were incubated with pure H-NS protein. In panels A to D, labeled DNAs were incubated with 0 (lanes 1), 12 (lanes 2), 18 (lanes 3), and 24 (lanes 4) ng of H-NS and with 24 ng of H-NS and a 62.5-fold excess of unlabeled competitor DNA (lanes 5). In panel E, labeled DNA was incubated with 0 (lane 1), 12 (lane 2), and 24 (lane 3) ng of H-NS and with 24 ng of H-NS and a 62.5-fold excess of unlabeled competitor DNA (lane 4). The spans of the promoter fragments used relative to the start codon were as follows: positions −306 to −83 for *tcpA*, positions −356 to −136 for *flrA*, positions −447 to −229 relative to VC2522 for *rpoN*, positions −272 to −19 for *hapA*, and positions −113 to +43 for VC1922.

cant binding affinity in the EMSA. The rationale for the *rpsM* ORF control was that though H-NS could bind to this sequence, such binding would not be relevant to transcription regulation and would provide a cutoff for distinguishing H-NS binding as a repressor versus nucleoid organization. In the ChIP analysis whose results are shown in Fig. 5, the *tcpA* promoter exhibited the highest H-NS occupancy, followed by *flrA* and *hapA*. The relative IP values obtained for VC1922 and *rpsM* were not considered indicative of H-NS transcription repression activity. According to these criteria, H-NS occupancy at the *rpoN* promoter was not significant under the experimental conditions used. Interestingly, deletion of *rpoS* resulted in higher H-NS promoter occupancy at the *tcpA*, *flrA*, and *hapA* promoters (Fig. 5B). Western blot analysis did not reveal differences in H-NS–FLAG expression between the wild-type and Δ*rpoS* strains, indicating that the observed increase in promoter occupancy is not due to an increase in H-NS–FLAG expression in the Δ*rpoS* mutant (Fig. 5C).

RpoS enhances the expression of IHF. Gene expression profiling of an Δ*rpoS* mutant of strain C7258 grown to the stationary phase revealed that the expression of IHF was downregulated in the mutant (unpublished results). Since IHF has been shown to enhance *tcpA* expression by binding to its promoter at a site that overlaps the H-NS binding site (52), we hypothesized that the expression of RpoS could diminish H-NS promoter occupancy at the *tcpA*, *flrA*, and *hapA* promoters by inducing the expression of IHF. Thus, we used qRT-PCR to determine the expression of *ihfA* and *ihfB* genes, encoding the IHF A and B subunits, respectively. As shown in Table 3, *ihfA* and *ihfB* were expressed in exponentially growing and late logarithmic cells at low levels but increased significantly in stationary-phase cells. The expression levels of *ihfA* and *ihfB* were reduced 8.2- and 4.2-fold in the Δ*rpoS* mutant, respectively. Lower expression levels of *ihfA* and *ihfB* were also observed in the Δ*hns* mutant, as expected from H-NS positively affecting the expression of RpoS (see Fig. 8) (49).

Integration host factor positively affects the expression of *flrA* and *rpoN*. Analysis of the *flrA* and *rpoN* promoters using Virtual Footprint software (http://www.prodoric.de/vfp/vfp_promoter.php) showed the presence of IHF binding sites with scores higher than those found at the *tcpA* promoter, which is enhanced by this regulator (52). Thus, we introduced an *ihfA* deletion in strains C7258 and AJB50 (Δ*rpoS*) and used qRT-PCR to assess the effect of RpoS and IHF on the expression of *flrA* and *rpoN*. As shown in Fig. 6, significantly less *flrA* and *rpoN* mRNA was detected in the *rpoS* and *ihfA* mutants. For both genes, the Δ*rpoS* Δ*ihfA* double mutant exhibited the lowest level of expression. To examine the role of IHF in H-NS occupancy at the *tcpA*, *flrA*, and *rpoN* promoters, the allele encoding H-NS–FLAG was also introduced in strains containing Δ*ihfA* and Δ*rpoS* Δ*ihfA* mutations. As shown in Fig. 7, higher promoter occupancies at the *tcpA* and *flrA* promoters were found in the *ihfA* mutant than in the

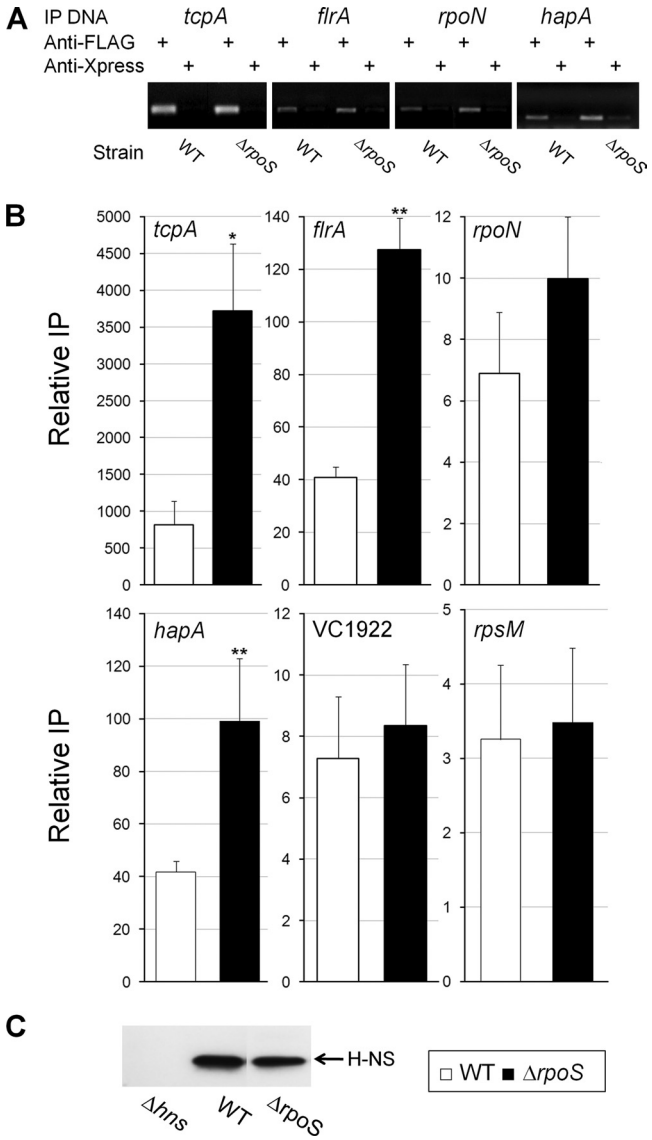

FIG 5 ChIP analysis of H-NS binding to different promoters. (A) Agarose gel electrophoresis of the PCR products obtained after ChIP using anti-FLAG and anti-Xpress (mock reaction) monoclonal antibodies. (B) Quantification of H-NS occupancy at the corresponding promoter in strains C7258HNS-FLAG (WT) and AJB50HNS-FLAG (Δ*rpoS*) by qPCR. Each value represents the mean for three experiments, and error bars indicate standard deviations (*, significantly different from that of the wild type [$P < 0.05$]; **, $P < 0.01$). (C) Detection of H-NS–FLAG protein expression in C7258HNS-FLAG (WT) and AJB50HNS-FLAG (Δ*rpoS*). In all experiments, *V. cholerae* strains were grown in TSB medium at 37°C to the stationary phase.

TABLE 3 Expression of IHF subunits in *V. cholerae* Δ*rpoS* and Δ*hns* mutants[a]

Strain	Relative expression of *ihfA* at:			Relative expression of *ihfB* at:		
	OD_{600} of 0.5	OD_{600} of 2.0	Stationary phase	OD_{600} of 0.5	OD_{600} of 2.0	Stationary phase
C7258Δ*lacZ* (WT)	0.75 ± 0.14	1.50 ± 0.28	78.77 ± 9.51	0.36 ± 0.03	0.71 ± 0.12	55.39 ± 5.12
AJB50Δ*lacZ* (Δ*rpoS*)	0.85 ± 0.10	1.52 ± 0.18	9.59* ± 1.39	0.48 ± 0.02	0.86 ± 0.09	13.34* ± 0.97
AJB80 (Δ*hns*)	1.48 ± 0.41	2.08 ± 0.61	39.52* ± 2.85	0.49 ± 0.09	0.83 ± 0.11	8.70* ± 1.84
AJB81 (Δ*rpoS* Δ*hns*)	1.05 ± 0.13	1.92 ± 0.50	6.16* ± 0.97	0.47 ± 0.06	0.87 ± 0.04	4.05* ± 1.84

[a] Each value represents the mean for at least three independent cultures ± the standard deviation. *, significantly different from that of the wild type [$P < 0.01$].

wild type. The Δ*rpoS* Δ*ihfA* double mutant exhibited the highest H-NS occupancies for *tcpA*, *flrA*, and *rpoN*, suggesting the occurrence of more than one mechanism involved in this process.

H-NS can negatively affect its occupancy of target promoters by enhancing RpoS. The data noted above revealed a regulatory pathway by which the expression of RpoS in the stationary phase could diminish H-NS occupancy of target promoters at which σ^S could initiate transcription (Fig. 5). In a previous study, we showed that H-NS positively affected the expression of *rpoS* by stabilizing its mRNA (49). To demonstrate that H-NS enhances RpoS protein expression, we compared the production levels of a chromosomally integrated *rpoS*-FLAG allele from its native transcription and translation signals in WT and Δ*hns* strains. As shown in Fig. 8, the Δ*hns* mutant expressed reduced RpoS-FLAG expression compared to the wild-type strain.

DISCUSSION

The general stress response regulator RpoS and the nucleoid structuring protein H-NS are global regulators known to affect intestinal colonization, virulence gene expression, and mucosal escape in the cholera bacterium (18, 27, 32, 35, 49). Here, we focus on the role of these proteins in the transcription of motility regulators *rpoN* and *flrA* as well as *hapA*, encoding HA/protease. Like other Gram-negative bacteria, *V. cholerae hns* mutants exhibit a slow-growth phenotype. It has been suggested that the inadequate overexpression of numerous cellular proteins and defective chromosome replication contribute to slow growth of *hns* mutants (1, 20, 24). In *E. coli*, RpoS and entire sets of RpoS-dependent genes are repressed by H-NS, and it has been shown that deletion of *hns* leads to deleterious overexpression of these genes in the exponential phase (3, 6, 19, 20). Our finding that deletion of *rpoS* partially suppressed the slow-growth phenotype of a *V. cholerae hns* mutant is consistent with the presence of an important set of genes in the cholera bacterium's genome under dual regulation by RpoS and H-NS. The fact that deletion of *rpoS* did not fully suppress the Δ*hns* slow-growth phenotype indicates that other cellular processes are compromised in the *hns* mutant. For instance, we observed that *V. cholerae hns* mutant cells appear elongated compared to wild-type cells, and their morphology was not suppressed by deletion of *rpoS*. This result is consistent with data showing that defective chromosome replication in *hns* mutants is independent of RpoS (1). Microscopic examination revealed that the Δ*hns* and Δ*rpoS* Δ*hns* mutants are both flagellated and similarly depressed for swimming. Thus, we suggest that the increase in swarm diameter observed in the Δ*rpoS* Δ*hns* double mutant compared to that of its Δ*hns* precursor (49) is a consequence of partial suppression of the Δ*hns* slow-growth phenotype.

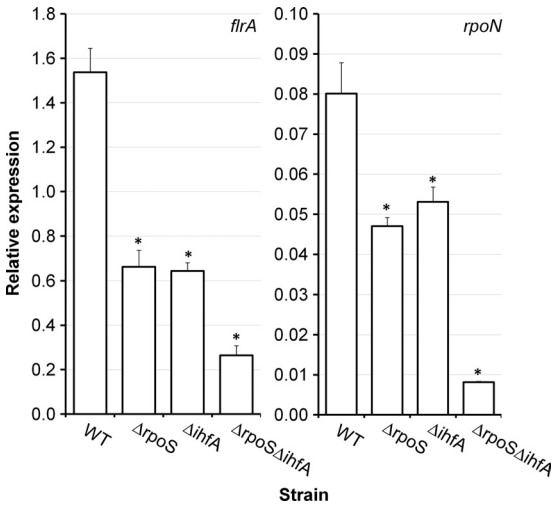

FIG 6 Role of integration host factor in the expression of *rpoN* and *flrA*. C7258 (WT), AJB50 (Δ*rpoS*), HX120 (Δ*ihfA*), and HX121 (Δ*rpoS* Δ*ihfA*) strains were grown with agitation in TSB medium at 37°C until the stationary phase, and the relative expression levels of *flrA* and *rpoN* were determined by qRT-PCR as described in Materials and Methods. Each value represents the mean for three experiments, and error bars indicate standard deviations (*, significantly different from that of the wild type [$P < 0.01$]).

In *V. cholerae*, RpoS activates *hapA* and enhances the expression of motility genes belonging to the class II, III, and IV hierarchies (35, 46, 57). We examined the role of RpoS and H-NS in the expression of *rpoN* and *flrA*, which control the expression of the class II, III, and IV hierarchy motility genes (42). In this study, we demonstrate that RpoS can enhance motility by positively affecting the expression of *rpoN* and *flrA* while H-NS acts as a repressor of these genes. These results suggest that RNAP containing σ^S can contribute to the transcription of *flrA* and *rpoN* in the stationary phase. Repression by H-NS was stronger at the *flrA* and *rpoN* promoters than at the *hapA* promoter. The difference between *flrA*, *rpoN*, and *hapA* is that while the first two promoters are transcribed by RNAP containing σ^{70} in exponentially growing cultures, the expression of *hapA* is tightly RpoS dependent and restricted to the stationary phase. The behavior of these promoters appears to be in agreement with studies suggesting that H-NS exhibits higher selectivity for inhibition of transcription initiated by RNAP containing σ^{70} (19–21, 54). Thus, we propose that participation of RNAP-σ^S in the transcription of *flrA* and *rpoN* in the stationary phase could render these promoters more resistant to repression by H-NS. As expected, a similar interplay between RpoS and H-NS was observed in the regulation of the downstream gene *flaA*, encoding the major *V. cholerae* flagellin. The observed regulation raises the question of why the *hns* mutant is less motile in spite of being flagellated and having elevated *flaA* expression. One possibility is that the altered cell morphology of this mutant

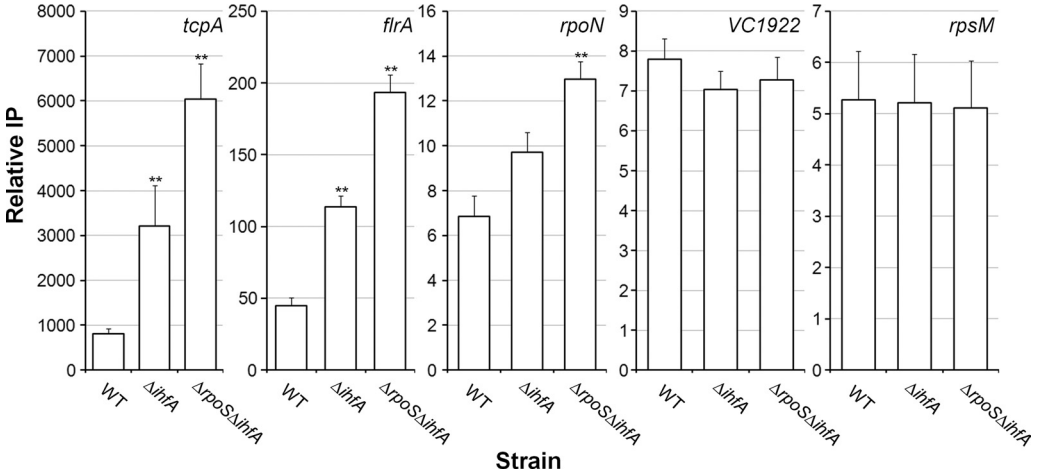

FIG 7 Effect of IHF on H-NS promoter occupancies. Strains C7258HNS-FLAG, HX120HNS-FLAG, and HX121HNS-FLAG were grown to the stationary phase in TSB medium at 37°C, and H-NS promoter occupancies were determined by ChIP and qPCR as described in Materials and Methods. Each value represents the mean for three experiments, and error bars indicate standard deviations (**, $P < 0.01$).

could indirectly hamper flagellum rotation and/or bacterial swimming speed. A second explanation, suggested by analogy to *E. coli*, is that H-NS could participate directly in torque generation by interacting with the switch complex proteins FliG and MotA (12). In this case, the lack of H-NS leads to a paralyzed flagellum.

Gel retardation assays indicated that H-NS can bind the *flrA*, *rpoN*, and *hapA* promoters with an affinity comparable to that of *tcpA*, a promoter known to be silenced by H-NS (37). H-NS is known to exhibit a broad specificity window for DNA binding that could be affected by the presence of other regulators. Thus, we conducted ChIP to determine H-NS occupancy at the *tcpA*, *flrA*, *rpoN*, and *hapA* promoters, using the promoter region of VC1922 and a sequence within the *rpsM* ORF as negative controls. According to our data, the highest H-NS occupancy was found for *tcpA*, followed by *flrA* and *hapA*. Very little H-NS occupancy was found at the *rpoN* promoter, suggesting that, at the time cells were collected for ChIP, other regulatory factors could prevent H-NS binding to this promoter. Deletion of *rpoS* significantly enhanced H-NS occupancy at the *tcpA*, *flrA*, and *hapA* promoters. The effect of RpoS on H-NS occupancy suggests a second manner by which the expression of σ^S can partially counteract H-NS repression. Sigma S has less affinity for the core polymerase than σ^{70}, with which it needs to compete for binding before it can access promoters (9). In addition, RNAP containing either σ^{70} or σ^S does not compete with H-NS for binding to promoter DNAs (45). Thus, we suggest that RpoS could diminish H-NS occupancy indirectly by inducing the expression of other *trans*-acting transcriptional regulators. IHF is known to alleviate H-NS silencing of *S. enterica hilA* (43), *E. coli csgD* (38), *Shigella flexneri vir* genes (41), and the bacteriophage Mu early promoter (56). In *V. cholerae*, IHF positively affects *tcpA* expression by binding to its promoter at a position that overlaps the H-NS binding site (52). Here, we show that the expression of RpoS in the stationary phase led to a significant increase in IHF expression. Moreover, we found that, similar to *tcpA* (52), IHF enhanced the expression of *flrA* and *rpoN*. The finding that deletion of both *ihfA* and *rpoS* diminished the expression of *flrA* and *rpoN* in an additive manner is consistent with the occurrence of more than one mechanism affecting the expression of these genes in the double mutant. Furthermore, H-NS occupancies at the *tcpA* and *flrA* promoters were significantly enhanced in the *ihfA* mutant compared to those in the wild-type strain.

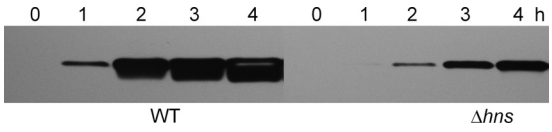

FIG 8 Regulation of RpoS (σ^S) expression by H-NS. C7258Δ*lacZ* RpoS-FLAG (WT) and AJB80RpoS-FLAG (Δ*hns*::km) strains were grown with agitation in TSB medium at 37°C to an OD_{600} of 2.0 (time zero). Then, samples were taken at 1-h intervals to determine the expression of RpoS-FLAG, as described in Materials and Methods.

It has been suggested that the open initiation complex formed with the promoter in RNAP-σ^{70} differs in architecture from that in RNAP-σ^3. The complex formed by RNAP-σ^{70} facilitates lateral oligomerization of H-NS by cooperative recruitment of H-NS molecules, leading to the formation of a repression loop (45). In contrast, the RNAP-σ^S open initiation complex does not promote H-NS oligomerization and exhibits H-NS-resistant transcription initiation (45). Consistent with this mechanism, the elevated promoter occupancies found in the Δ*rpoS* Δ*ihfA* double mutant could result from the absence of IHF, required to displace H-NS from its binding site, and the formation of only RNAP-σ^{70} open initiation complexes that favor H-NS oligomerization along DNA. In addition, deletion of *rpoS* could lead to enhanced activity of σ^{70} (19–21), favoring a higher association between H-NS and promoter DNA. Also, our finding that H-NS exerts weaker repression at the *hapA* promoter is in agreement with the above-mentioned model for H-NS promoter selectivity.

Consistent with our previous finding that H-NS enhances *rpoS* mRNA stability (49), here we show that H-NS positively affected the expression of RpoS at the protein level. This regulation could generate a negative regulatory loop in which elevated RpoS expression could diminish H-NS occupancy at target promoters that could be transcribed using RNAP-σ^S by activating the expression of IHF or other *trans*-acting regulatory factors.

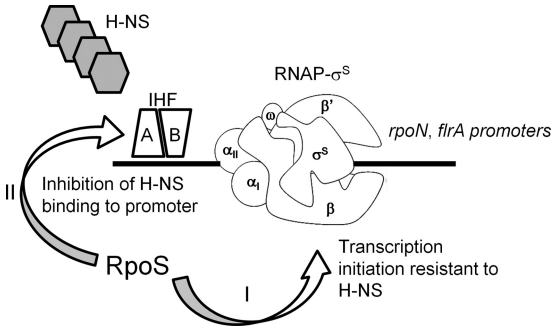

FIG 9 Model for RpoS regulation of motility in *V. cholerae*. The expression of RpoS in the stationary phase enhances *rpoN* and *flrA* transcription by two parallel mechanisms. In mechanism I, RNAP-σ^S can initiate transcription at the *rpoN* and *flrA* promoters. Transcription initiation by RNAP-σ^S is more resistant to H-NS repression. In mechanism II, RpoS diminishes H-NS occupancy at the *rpoN* and *flrA* promoters indirectly by enhancing the expression of IHF, which could compete with H-NS for binding to DNA.

Based on our results, we propose a model for the interplay between RpoS and H-NS at *V. cholerae* promoters that control motility (Fig. 9). Briefly, H-NS binds to the *flrA* and *rpoN* promoters to repress transcription. RpoS is expressed in the stationary phase, and RNAP-σ^S contributes to the transcription of *flrA* and *rpoN*, rendering these promoters more resistant to H-NS repression (Fig. 9, I). In addition, the expression of RpoS can indirectly attenuate H-NS-mediated repression of *flrA* and *rpoN* by inducing the expression of IHF (Fig. 9, II). IHF acts by displacing H-NS from its binding site to enhance transcription of *flrA* and *rpoN*, as described for the *tcpA* promoter (52). Our data provide an explanation for RpoS regulation of motility and mucosal escape (35). Moreover, RpoS was shown to be required for intestinal colonization in an El Tor biotype strain (32). Our results also suggest that RpoS could favor colonization by diminishing H-NS repression of motility and *tcpA* expression, which are required to establish infection (22, 47).

ACKNOWLEDGMENTS

This study was partially supported by National Institutes of Health research grants GM008248 and AI081039 to A.J.S.

We are grateful to Jian-He Wu for her general assistance in the conduction of this research and the analysis of RpoS-FLAG expression.

REFERENCES

1. **Atlung T, Hansen FG.** 2002. Effect of different concentrations of H-NS protein on chromosome replication and the cell cycle in *Escherichia coli.* J. Bacteriol. **184**:1843–1850.
2. **Atlung T, Ingmer H.** 1997. H-NS: a modulator of environmentally regulated gene expression. Mol. Microbiol. **24**:7–17.
3. **Barth M, Marschall C, Muffler A, Fischer D, Hengge-Aronis R.** 1995. Role for the histone-like protein H-NS in growth phase-dependent and osmotic regulation of σ^S and many σ^S-dependent genes in *Escherichia coli.* J. Bacteriol. **177**:3455–3464.
4. **Benitez JA, Silva AJ, Finkelstein RA.** 2001. Environmental signals controlling production of hemagglutinin/protease in *Vibrio cholerae.* Infect. Immun. **69**:6549–6553.
5. **Benitez JA, et al.** 1997. Adherence of *Vibrio cholerae* to cultured differentiated human intestinal cells: an *in vitro* colonization model. Infect. Immun. **65**:3474–3477.
6. **Bouvier J, et al.** 1998. Interplay between global regulators of *Escherichia coli*: effect of RpoS, Lrp and H-NS on transcription of the gene *osmC.* Mol. Microbiol. **28**:971–980.
7. **Brescia CC, Kaw MK, Sledjeski DD.** 2004. The DNA binding protein H-NS binds to and alters the stability of RNA *in vitro* and *in vivo.* J. Mol. Biol. **339**:505–514.
8. **Cerdan R, et al.** 2003. Crystal structure of the N-terminal dimerization domain of VicH, the H-NS-like protein of *Vibrio cholerae.* J. Mol. Biol. **334**:179–185.
9. **Colland F, Fujita N, Ishihama A, Kolb A.** 2002. The interaction between sigma S, the stationary phase sigma factor, and the core enzyme of Escherichia coli RNA polymerase. Genes Cells **7**:233–247.
10. **Dame RT, Wyman C, Goosen N.** 2001. Structural basis for preferential binding of H-NS to curved DNA. Biochimie **83**:231–234.
11. **De Lorenzo V, Eltis L, Kessler B, Timmis KN.** 1993. Analysis of the *Pseudomonas* gene products using *lacI*^{q}/*Ptrp-lac* plasmids and transposons that confer conditional phenotypes. Gene **123**:17–24.
12. **Donato GM, Kawula TH.** 1998. Enhanced binding of altered H-NS to flagellar rotor protein FliG causes increased flagellar rotation speed and hypermotility in *Escherichia coli.* J. Biol. Chem. **273**:24030–24036.
13. **Donnenberg MS, Kaper JB.** 1991. Construction of an eae deletion mutant of enteropathogenic *Escherichia coli* by using a positive selection suicide vector. Infect. Immun. **59**:4310–4317.
14. **Dorman CJ.** 2004. H-NS: a universal regulator for a dynamic genome. Nat. Rev. Microbiol. **2**:391–400.
15. **Dorman CJ, Deighan P.** 2003. Regulation of gene expression by histone-like proteins in bacteria. Curr. Opin. Genet. Dev. **13**:179–184.
16. **Finkelstein RA.** 1992. Cholera enterotoxin (choleragen): a historical perspective, p 155–187. *In* Barua D, Greenough WB (ed), Cholera. Plenum Medical Book Company, New York, NY.
17. **Finkelstein RA, Boesman-Finkelstein M, Chang Y, Häse CC.** 1992. *Vibrio cholerae* hemagglutinin/protease, colonial variation, virulence, and detachment. Infect. Immun. **60**:472–478.
18. **Ghosh A, Paul K, Chowdhury R.** 2006. Role of the histone-like nucleoid structuring protein in colonization, motility, and bile-dependent repression of virulence gene expression in *Vibrio cholerae.* Infect. Immun. **74**:3060–3064.
19. **Hengge-Aronis R.** 1999. Interplay of global regulators and cell physiology in the general stress response of *Escherichia coli.* Curr. Opin. Microbiol. **2**:148–152.
20. **Hengge-Aronis R.** 2002. Signal transduction and regulatory mechanisms involved in control of the Sigma S (RpoS) subunit of RNA polymerase. Microbiol. Mol. Biol. Rev. **66**:373–395.
21. **Hengge-Aronis R.** 2002. Stationary phase gene regulation: what makes an *Escherichia coli* promoter σ^S-selective? Curr. Opin. Microbiol. **5**:591–595.
22. **Herrington DA, et al.** 1988. Toxin, the toxin co-regulated pili and the *toxR* regulon are essential for *Vibrio cholerae* pathogenesis in humans. J. Exp. Med. **168**:1487–1492.
23. **Hommais F, et al.** 2001. Large-scale monitoring of pleiotropic regulation of gene expression by the prokaryotic nucleoid-associated protein, H-NS. Mol. Microbiol. **40**:20–36.
24. **Kaidow A, Wachi M, Nakamura J, Magae J, Nagai K.** 1995. Anucleate cell production by Escherichia coli hns mutant lacking a histone like protein, H-NS. J. Bacteriol. **177**:3589–3592.
25. **Kaper JB, Morris G, Jr, Levine MM.** 1995. Cholera. Clin. Microbiol. Rev. **8**:48–86.
26. **Klose KE, Mekalanos JJ.** 1998. Differential expression of multiple flagellins in *Vibrio cholerae.* J. Bacteriol. **180**:303–316.
27. **Krishnan HH, Ghosh A, Paul K, Chowdhury R.** 2004. Effect of anaerobiosis on expression of virulence factors in *Vibrio cholerae.* Infect. Immun. **72**:3961–3967.
28. **Lang B, et al.** 2007. High-affinity DNA binding sites for H-NS provide a molecular basis for selective silencing within proteobacterial genomes. Nucleic Acids Res. **35**:6330–6337.
29. **Liang W, Pascual-Montano A, Silva AJ, Benitez JA.** 2007. The cyclic AMP receptor protein modulates quorum sensing, motility and multiple genes that affect intestinal colonization in *Vibrio cholerae.* Microbiology **153**:2964–2975.
30. **Lucchini S, et al.** 2006. H-NS mediates the silencing of laterally acquired genes in bacteria. PLoS Pathog. **2**:e81.
31. **Marcus H, Ketley JM, Kaper JB, Holmes RK.** 1990. Effect of DNAse production, plasmid size and restriction barrier on transformation of *Vibrio cholerae* by electroporation and osmotic shock. FEMS Microbiol. Lett. **68**:149–154.
32. **Merrell DS, Tischler AD, Lee SH, Camilli A.** 2000. *Vibrio cholerae* requires *rpoS* for efficient intestinal colonization. Infect. Immun. **68**:6691–6696.

33. **Miller JH.** 1971. Experiments in molecular genetics. Cold Spring Harbor Laboratory Press, Cold Spring Harbor, NY.
34. **Navarre WW, et al.** 2006. Selective silencing of foreign DNA with low GC content by the H-NS protein in *Salmonella.* Science **313**:236–238.
35. **Nielsen AT, et al.** 2006. RpoS controls the *Vibrio cholerae* mucosal escape response. PLoS Pathog. **2**:e109.
36. **Nye MB, Taylor RK.** 2003. *Vibrio cholerae* H-NS domain structure and function with respect to transcriptional repression of ToxR regulon genes reveals differences among H-NS family members. Mol. Microbiol. **50**: 427–444.
37. **Nye MB, Pfau JD, Skorupski K, Taylor RK.** 2000. *Vibrio cholerae* H-NS silences virulence gene expression at multiple steps in the ToxR regulatory cascade. J. Bacteriol. **182**:4295–4303.
38. **Ogasawara H, Yamada K, Kori A, Yamamoto K, Ishihama A.** 2010. Regulation of the *Escherichia coli csgD* promoter: interplay between five transcription factors. Microbiology **156**:2470–2483.
39. **Oshima T, Ishikawa S, Kurokawa K, Aiba H, Ogasawara N.** 2006. *Escherichia coli* histone-like protein H-NS preferentially binds to horizontally acquired DNA in association with RNA polymerase. DNA Res. **13**: 141–153.
40. **Owen-Hughes TA, et al.** 1992. The chromatin-associated protein H-NS interacts with curved DNA to influence DNA topology and gene expression. Cell **71**:255–265.
41. **Porter ME, Dorman CJ.** 1997. Positive regulation of *Shigella flexneri* virulence genes by integration host factor. J. Bacteriol. **179**:6537–6550.
42. **Prouty MG, Correa NE, Klose KE.** 2001. The novel sigma 54- and sigma 28-dependent flagellar gene transcription hierarchy of *Vibrio cholerae.* Mol. Microbiol. **39**:1595–1609.
43. **Queiroz MH, Madrid C, Paytubi S, Balsalobre C, Juarez A.** 2011. Integration host factor alleviates H-NS silencing of the *Salmonella enterica* serovar Typhimurium master regulator of SP11, *hilA*. Microbiology [Epub ahead of print.] doi:10.1099/mic.0.049197-0.
44. **Rothmel RD, Shinabarger D, Parsek M, Aldrich T, Chakrabarty AM.** 1991. Functional analysis of the *Pseudomonas putida* regulatory protein CatR: transcriptional studies and determination of the CatR DNA binding site by hydroxyl-radical footprinting. J. Bacteriol. **173**:4717–4724.
45. **Shin M, et al.** 2005. DNA looping-mediated repression by histone-like protein H-NS: specific requirement of Eσ^{70} as a cofactor for looping. Genes Dev. **19**:2388–2398.
46. **Silva AJ, Benitez JA.** 2004. Transcriptional regulation of *Vibrio cholerae* hemagglutinin/protease by the cyclic AMP receptor protein and RpoS. J. Bacteriol. **186**:6374–6382.
47. **Silva AJ, Leitch GJ, Camilli A, Benitez JA.** 2006. Contribution of hemagglutinin/protease and motility to the pathogenesis of El Tor biotype cholera. Infect. Immun. **74**:2072–2079.
48. **Silva AJ, Pham K, Benitez JA.** 2003. Hemagglutinin/protease expression and mucin gel penetration in El Tor biotype *Vibrio cholerae.* Microbiology **149**:1883–1891.
49. **Silva AJ, Zafar Sultan S, Liang W, Benitez JA.** 2008. Role of the histone-like nucleoid structuring protein (H-NS) in the regulation of RpoS and RpoS-dependent genes in *Vibrio cholerae.* J. Bacteriol. **190**:7335–7345.
50. **Spurio R, Falconi M, Brandi A, Pon CL, Gualerzi CO.** 1997. The oligomeric structure of the nucleoid protein H-NS is necessary for recognition of intrinsically curved DNA and for DNA binding. EMBO J. **16**: 1795–1805.
51. **Stonehouse EA, Hulbert RR, Nye MB, Skorupski K, Taylor RK.** 2011. H-NS binding and repression of the ctx promoter in *Vibrio cholerae.* J. Bacteriol. **193**:979–988.
52. **Stonehouse E, Kovacikova G, Taylor RK, Skorupski K.** 2008. Integration host factor positively regulates virulence gene expression in *Vibrio cholerae.* J. Bacteriol. **190**:4736–4748.
53. **Tendeng C, et al.** 2000. Isolation and characterization of *vicH*, encoding a new pleiotropic regulator in *Vibrio cholerae.* J. Bacteriol. **182**:2026–2032.
54. **Typas A, Becker G, Hengge R.** 2007. The molecular basis of selective promoter activation by the σ^S subunit of RNA polymerase. Mol. Microbiol. **63**:1296–1306.
55. **Ueguchi C, Mizuno T.** 1993. The *Escherichia coli* nucleoid protein H-NS functions directly as a transcriptional repressor. EMBO J. **12**:1039–1046.
56. **Van Ulsen P, Hillebrant M, Zulianello L, van de Putte P, Goosen N.** 1996. Integration host factor alleviates the H-NS-mediated repression of the early promoter of bacteriophage Mu. Mol. Microbiol. **3**:567–578.
57. **Wang H, Wu J-H, Ayala JC, Benitez JA, Silva AJ.** 2011. Interplay among cyclic diguanylate, HapR, and the general stress response regulator (RpoS) in the regulation of *Vibrio cholerae* hemagglutinin/protease. J. Bacteriol. **193**:6529–6538.
58. **Yildiz FH, Schoolnik GK.** 1998. Role of *rpoS* in stress survival and virulence of *Vibrio cholerae.* J. Bacteriol. **180**:773–784.
59. **Yu RR, DiRita VJ.** 2002. Regulation of gene expression in *Vibrio cholerae* by *toxT* involves both antirepression and RNA polymerase stimulation. Mol. Microbiol. **43**:119–134.
60. **Zhu J, et al.** 2002. Quorum-sensing regulators control virulence gene expression in *Vibrio cholerae.* Proc. Natl. Acad. Sci. U. S. A. **99**:3129–3134.